Degrees-of-Freedom Region of Time Correlated MISO Broadcast Channel with Perfect Delayed CSIT and Asymmetric Partial Current CSIT

Chenxi Hao and Bruno Clerckx
Communication and Signal Processing Group, Department of Electrical and Electronic Engineering
Imperial College London, United Kingdom
Email: {chenxi.hao10,b.clerckx}@imperial.ac.uk

***Abstract*—The impact of imperfect CSIT on the degrees of freedom (*DoF*) of a time correlated MISO Broadcast Channel has drawn a lot of attention recently. Maddah-Ali and Tse have shown that the completely stale CSIT still benefit the *DoF*. In very recent works, Yang et al. have extended the results by integrating the partial current CSIT for a two-user MISO broadcast channel. However, those researches so far focused on a symmetric case. In this contribution, we investigate a more general case where the transmitter has knowledge of current CSI of both users with unequal qualities. The essential ingredient in our work lies in the way to multicast the overheard interference to boost the *DoF*. The optimal *DoF* region is simply proved and its achievability is shown using a novel transmission scheme assuming an infinite number of channel uses.**

I. Introduction

Maddah-Ali and Tse have recently investigated the *DoF* region of Broadcast Channels with perfect delayed (completely stale) CSIT [1]. They have shown that the per-user optimal *DoF* is $\frac{2}{3}$ in a two-user setup and proposed a simple transmission scheme (denoted as MAT scheme in the sequel) to achieve that *DoF* over 3 time slots. In the first and second slot, each user in turn receives the desired signal and overhears the unwanted signal, while in the third slot, the sum of the overheard interference is transmitted to enable the decoding of the desired signal at each receiver.

Those results have recently been extended to a more general setup with perfect delayed CSIT and partial current CSIT [2] [3]. An optimal combining of perfect delayed CSIT and partial current CSIT is obtained to bridge the *DoF* of [1] with outdated CSIT and the *DoF* achievable with zero-forcing beamforming with perfect current CSIT. However results in [2] and [3] are limited to a symmetric case where the transmitter has access to both users' CSI with the same accuracy.

In [4], an outer-bound on the *DoF* region was given under the settings that the transmitter and receivers have multiple antennas and perfect delayed CSIT. The authors of [5] and [6] studied the same settings but without CSIT. Moreover, In [7][8], the optimal sum *DoF* of $\frac{3}{2}$ was derived when the CSIT of one user is perfect but it is out-dated for the other user.

In this paper, we further extend the analysis by considering a more general asymmetric scenario where the qualities of current CSI of users' channels available at the transmitter are unequal. Our contributions are summarized as follows:

1) the transmission schemes derived for the symmetric case are shown to incur a *DoF* loss in an asymmetric scenario,
2) the *DoF* region obtained in [2] is extended to the asymmetric scenario and is expressed as a function of two parameters representing the accuracy of CSIT of each user's channel,
3) a novel transmission scheme (that subsumes the scheme in [2] in the symmetric case) is derived and shown to achieve the *DoF* region in the limit of an infinite number of channel uses.

At the time of submission, we have been informed of another independent work, also in submission, that addresses the same problem [9]. Interestingly, both works derive the same achievable *DoF* region using different approaches and its achievability is demonstrated using two different transmission strategies.

The rest of this paper is organized as follows. The system model is introduced in Section II and the *DoF* region is derived in Section III. The limitations of the transmission schemes designed for symmetric partial current CSIT are discussed in Section IV and a novel transmission scheme achieving the optimal *DoF* region in the setting of asymmetric partial current CSIT is introduced. Section V concludes the paper.

The following notations are used throughout the paper. Upper letters in bold font represent matrices whereas bold lower letters stand for vectors. However, symbol not in bold font represents a scalar. $(\cdot)^T$ and $(\cdot)^H$ represent the transpose and conjugate transpose of a matrix or vector respectively. $\mathbf{h}^{\perp}$ denotes the orthogonal space of channel vector $\mathbf{h}$. $\mathcal{E}[\cdot]$ refers to the expectation of a random variable, vector or matrix. $\|\cdot\|$ is the norm of a vector. $f(P) \sim P^B$ corresponds to $\lim_{P\to\infty} \frac{\log f(P)}{\log P} = B$, where P refers to SNR throughout the paper and logarithms are in base 2.

II. System Model

We consider a two-user Broadcast Channel with two transmit antennas and one antenna per user. $\mathbf{h}_t$ and $\mathbf{g}_t$ are the channel states at time slot t of user 1 and user 2 respectively. Denoting the transmit signal vector as $\mathbf{s}_t$, subject to a transmit power constraint $\mathcal{E}\left[\|\mathbf{s}_t\|^2\right] \leq P$, the observations at receiver 1

and 2, y_t and z_t respectively, can be written at time slot t as

$$y_t = \mathbf{h}_t^H \mathbf{s}_t + \epsilon_{t,1} \quad (1)$$

$$z_t = \mathbf{g}_t^H \mathbf{s}_t + \epsilon_{t,2}, \quad (2)$$

where $\epsilon_{t,1}$ and $\epsilon_{t,2}$ are unit power AWGN noise. Signal vector $\mathbf{s}_t$ is expressed as a function of the symbol vectors for user 1 and user 2, denoted as $\mathbf{u}_t$ and $\mathbf{v}_t$ respectively. $\mathbf{u}_t$ is a two-element symbol vector containing $u_{t,1}$ and $u_{t,2}$. $\mathbf{v}_t$ is defined similarly and is composed of $v_{t,1}$ and $v_{t,2}$. The power allocated to symbol $u_{t,1}$ is stated as $P_{u_{t,1}}$ while the rate achieved by $u_{t,1}$ is $R_{u_{t,1}}$. As $\mathbf{u}_t = [u_{t,1}, u_{t,2}]^T$, the power and rate of $\mathbf{u}_t$ are expressed as $P_{\mathbf{u}_t} = P_{u_{t,1}} + P_{u_{t,2}}$ and $R_{\mathbf{u}_t} = R_{u_{t,1}} + R_{u_{t,2}}$. These notations are applicable to $\mathbf{v}_t$, $v_{t,1}$ and $v_{t,2}$. For the sake of convenience, in a few instances, we denote the rate of each symbol or symbol vector by the pre-log factor (ignoring $\log P$).

The channel state information $\mathbf{h}_t$ and $\mathbf{g}_t$ are supposed to be mutually independent and identically distributed with zero mean and unit covariance matrix ($\mathcal{E}\left[|\mathbf{h}_t^H \mathbf{g}_t|^2\right] = 0$ and $\mathcal{E}\left[\mathbf{h}_t \mathbf{h}_t^H\right] = \mathbf{I}_2$). At any given time slot t, the transmitter and each user have perfect global knowledge of the channel states from time slot 0 to $t-1$, i.e. $\mathbf{h}_{0,1,\cdots,t-1}$ and $\mathbf{g}_{0,1,\cdots,t-1}$. Moreover, the transmitter can predict the current channel state of each user. The estimated channels are denoted as $\hat{\mathbf{h}}_t$ and $\hat{\mathbf{g}}_t$, with the corresponding error vectors written as $\tilde{\mathbf{h}}_t = \mathbf{h}_t - \hat{\mathbf{h}}_t$ and $\tilde{\mathbf{g}}_t = \mathbf{g}_t - \hat{\mathbf{g}}_t$. $\tilde{\mathbf{h}}_t$ and $\tilde{\mathbf{v}}_t$ have the variances denoted as $\mathcal{E}\left[\parallel \tilde{\mathbf{h}}_t \parallel^2\right] = \sigma_1^2$ and $\mathcal{E}\left[\parallel \tilde{\mathbf{g}}_t \parallel^2\right] = \sigma_2^2$, respectively. In the general asymmetric scenario under interest, the transmitter has unequal accuracy of the current CSI for each user, with the accuracy of the each current CSIT obtained according to

$$\alpha_k \triangleq \lim_{P\to\infty} -\frac{\log \sigma_k^2}{\log P}, k = 1, 2. \quad (3)$$

In other words, $\mathcal{E}\left[\parallel \tilde{\mathbf{h}}_t \parallel^2\right] \sim P^{-\alpha_1}$ and $\mathcal{E}\left[\parallel \tilde{\mathbf{g}}_t \parallel^2\right] \sim P^{-\alpha_2}$. α_1 and α_2 are supposed to vary in the range of $[0, 1]$, where $\alpha_k = 0$ represents no CSIT whereas $\alpha_k = 1$ stands for perfect CSIT. Throughout the paper, we assume $\alpha_1 \leq \alpha_2$ without loss of generality. Moreover, it is important to note the relationship $\mathcal{E}\left[|\mathbf{h}^H \hat{\mathbf{h}}^\perp|^2\right] \sim P^{-\alpha_1}$ and $\mathcal{E}\left[|\mathbf{g}^H \hat{\mathbf{g}}^\perp|^2\right] \sim P^{-\alpha_2}$.

III. *DoF* Region with Asymmetric Partial Current CSIT

Theorem 1: In the two-user MISO Broadcast Channel with perfect delayed CSIT and asymmetric partial current CSIT, the optimal *DoF* region is characterized by

$$\{d_1 \leq 1; d_2 \leq 1; d_1 + 2d_2 \leq 2 + \alpha_2; 2d_1 + d_2 \leq 2 + \alpha_1\} \quad (4)$$

A sketch of the proof will be given in the Appendix. The *DoF* region is illustrated in Figure 1. As shown, the outer-bound is a polygon composed of the points $(1, \alpha_1)$, $(\alpha_2, 1)$ and $\left(\frac{2+2\alpha_1-\alpha_2}{3}, \frac{2+2\alpha_2-\alpha_1}{3}\right)$. When α_1 is fixed, the intersection point which maximizes the sum *DoF* moves as α_2 increases. However, the intersection point goes outside the valid region as shown by the circle point in Figure 1 when $2\alpha_2 - \alpha_1 > 1$. In this case, the region is only formed by $(1, \alpha_1)$, $\left(\frac{1+\alpha_1}{2}, 1\right)$. Also, the point that achieves the maximum sum *DoF* returns to the triangle point (see Figure 1) achieved by taking $2\alpha_2 - \alpha_1 = 1$. When $\alpha_1 = \alpha_2$, the *DoF* region boils down to that of [2] as shown by the diamond point, suggesting that scheme II in [2] achieves a subset of the asymmetric region. Moreover, when $\alpha_1 = \alpha_2 = 0$, the region further boils down to the region achieved by MAT scheme in [1].

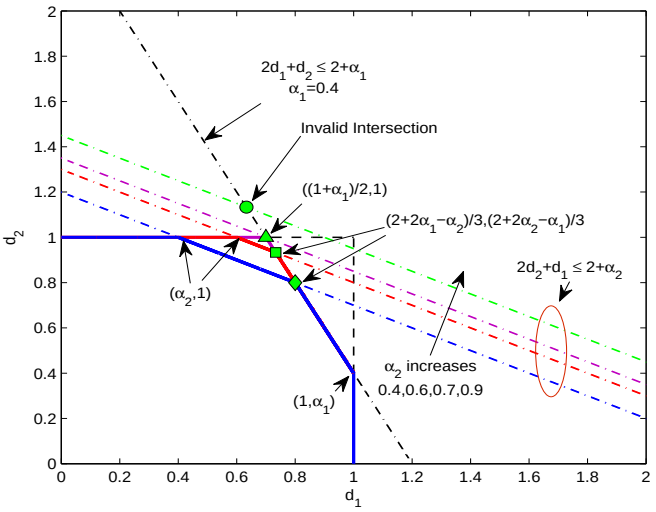

Fig. 1: DoF region with asymmetric partial current CSIT

IV. Achievability

A. Limitation of scheme II in [2]

Following the system model defined in Section II, we briefly review the transmission scheme II as proposed in [2] and identify the limitations of that scheme in an asymmetric configuration. The transmit signal and the received signal at each user at first time slot write as

$$\mathbf{s}_1 = \left[\hat{\mathbf{g}}_1^\perp, \hat{\mathbf{g}}_1\right] \mathbf{u}_1 + \left[\hat{\mathbf{h}}_1^\perp, \hat{\mathbf{h}}_1\right] \mathbf{v}_1, \quad (5)$$

$$y_1 = \mathbf{h}_1^H \hat{\mathbf{g}}_1^\perp u_{1,1} + \mathbf{h}_1^H \hat{\mathbf{g}}_1 u_{1,2} + \eta_{1,1} + \epsilon_{1,1}, \quad (6)$$

$$z_1 = \eta_{1,2} + \mathbf{g}_1^H \hat{\mathbf{h}}_1^\perp v_{1,1} + \mathbf{g}_1^H \hat{\mathbf{h}}_1 v_{1,2} + \epsilon_{1,2}, \quad (7)$$

where $P_{u_{1,1}} = P_{v_{1,1}} = P$ and $P_{u_{1,2}} = P^{1-\alpha_2}$, $P_{v_{1,2}} = P^{1-\alpha_1}$. $\eta_{1,1}$ (resp. $\eta_{1,2}$) represents the overheard interference generated at receiver 1 (resp. 2) at slot 1 and is expressed as

$$\eta_{1,1} = \mathbf{h}_1^H \hat{\mathbf{h}}_1^\perp v_{1,1} + \mathbf{h}_1^H \hat{\mathbf{h}}_1 v_{1,2}, \quad (8)$$

$$\eta_{1,2} = \mathbf{g}_1^H \hat{\mathbf{g}}_1^\perp u_{1,1} + \mathbf{g}_1^H \hat{\mathbf{g}}_1 u_{1,2}. \quad (9)$$

By integrating the current CSIT in the precoding procedure to $\mathbf{u}_1$, $\eta_{1,1}$ and $\eta_{1,2}$ are received with the power of $P^{1-\alpha_1}$ and $P^{1-\alpha_2}$ respectively since $\hat{\mathbf{h}}_1$ and $\hat{\mathbf{g}}_1$ have the respective quality of α_1 and α_2. As both overheard interferences have reduced power, the resource can be saved when multicasting them separately and sequentially at slot 2 and 3. The transmission and receive signals at slot 2 and 3 are expressed as

$$\mathbf{s}_2 = [\hat{\eta}_{1,1}, 0]^T + \hat{\mathbf{g}}_2^\perp u_2 + \hat{\mathbf{h}}_2^\perp v_2, \quad (10)$$

$$y_2 = h_{2,1}^* \hat{\eta}_{1,1} + \mathbf{h}_2^H \hat{\mathbf{g}}_2^\perp u_2 + \mathbf{h}_2^H \hat{\mathbf{h}}_2^\perp v_2 + \epsilon_{2,1}, \quad (11)$$

$$z_2 = g_{2,1}^* \hat{\eta}_{1,1} + \mathbf{g}_2^H \hat{\mathbf{g}}_2^\perp u_2 + \mathbf{g}_2^H \hat{\mathbf{h}}_2^\perp v_2 + \epsilon_{2,2}, \quad (12)$$

$$\mathbf{s}_3 = [\hat{\eta}_{1,2}, 0]^T + \hat{\mathbf{g}}_3^{\perp} u_3 + \hat{\mathbf{h}}_3^{\perp} v_3, \quad (13)$$

$$y_3 = h_{3,1}^* \hat{\eta}_{1,2} + \mathbf{h}_3^H \hat{\mathbf{g}}_3^{\perp} u_3 + \mathbf{h}_3^H \hat{\mathbf{h}}_3^{\perp} v_3 + \epsilon_{3,1}, \quad (14)$$

$$z_3 = g_{3,1}^* \hat{\eta}_{1,2} + \mathbf{g}_3^H \hat{\mathbf{g}}_3^{\perp} u_3 + \mathbf{g}_3^H \hat{\mathbf{h}}_3^{\perp} v_3 + \epsilon_{3,2}, \quad (15)$$

where, $\hat{\eta}_{t,1}$ and $\hat{\eta}_{t,2}$ are quantized versions of overheard interference with the quantization rate of $1-\alpha_1$ and $1-\alpha_2$ respectively. u_2 and v_2 are new symbols at slot 2 intended to user 1 and user 2 respectively. Similarly, u_3 and v_3 are defined at slot 3. The power allocated to each symbols in (10) and (13) are $P_{\hat{\eta}_{1,1}}{=}P_{\hat{\eta}_{1,2}}{=}P$, $P_{u_2}{=}P_{v_2}{=}P^{\alpha_1}$ and $P_{u_3}{=}P_{v_3}{=}P^{\alpha_2}$.

At each receiver, $\hat{\eta}_{1,1}$ and $\hat{\eta}_{1,2}$ are decoded at the first stage of SIC by treating all the other symbols as noise. At high SNR, $\hat{\eta}_{1,1}$ and $\hat{\eta}_{1,2}$ can be decoded at both receiver with the same rate as their respective quantization rate. Then $\hat{\eta}_{1,1}$ (resp. $\hat{\eta}_{1,2}$) can be employed to cancel the overheard interference $\eta_{1,1}$ (resp. $\eta_{1,2}$) and provide another independent observation to z_1 (resp. y_1). Consequently, $\mathbf{u}_1$ and $\mathbf{v}_1$ achieve the rate of $2-\alpha_2$ and $2-\alpha_1$, respectively. At slot 2, u_2 (resp. v_2) is drown by the noise in z_2 (resp. y_2) so that user 1 (resp. user 2) can decode u_2 (resp. v_2) without interference, thus, $R_{u_2}{=}R_{v_2}{=}\alpha_1$. At slot 3, the limitation rises because $\mathbf{h}_3^H \hat{\mathbf{h}}_3^{\perp} v_3$ is overheard by user 1 with the power of P^{Δ}, which is larger than the noise level. Then, u_3 is decoded by treating $\mathbf{h}_3^H \hat{\mathbf{h}}_3^{\perp} v_3$ as noise so that the rate of u_3 is restricted to α_1 while $R_{v_3}{=}\alpha_2$. To sum up, the *DoF* of each user's symbols is $\left(\frac{2+2\alpha_1-\alpha_2}{3}, \frac{2+\alpha_2}{3}\right)$. However, this *DoF* satisfies (4) and lies within the *DoF* region. It is outperformed by the intersection point $\left(\frac{2+2\alpha_1-\alpha_2}{3}, \frac{2+2\alpha_2-\alpha_1}{3}\right)$ and user 2 incurs a *DoF* loss of $\frac{\Delta=\alpha_2-\alpha_1}{3}$. The loss vanishes in the symmetric case as $\alpha_1{=}\alpha_2{=}\alpha$, where the above scheme achieves the optimal bound [2].

To boost up the *DoF* achieved at slot 3, the overheard interference $\mathbf{h}_3^H \hat{\mathbf{h}}_3^{\perp} v_3$ can be removed via retransmission at slot 4. However, since v_3 is decodable by user 2 at slot 3, this retransmission is wasteful for user 2. To make the retransmission efficient for both users, we compose $\mathbf{v}_3$ of $v_{3,1}$ and $v_{3,2}$ as a symbol vector rather than a single symbol. $v_{3,1}$ is precoded and allocated with the power same as that of v_3, $v_{3,2}$ is transmitted with power P^{Δ} so that the power of $\mathbf{h}_3^H \hat{\mathbf{h}}_3^{\perp} \mathbf{v}_3$ is not enhanced compared to $\mathbf{h}_3^H \hat{\mathbf{h}}_3^{\perp} v_3$. After receiving and decoding the quantized overheard interference, user 1 can remove $\mathbf{h}_3^H \hat{\mathbf{h}}_3^{\perp} \mathbf{v}_3$ while user 2 can decode both $v_{3,1}$ and $v_{3,2}$.

Accordingly, as long as one user overhears interference, the retransmission of the overheard interference is efficient in improving the *DoF* if we make the overheard interference composed of two symbols. Based on this observation, we derive a novel transmission scheme in the next section.

B. Building Blocks of a New Transmission Scheme

We identify important building blocks of a new transmission scheme that achieves the asymmetric *DoF* region of Theorem 1. Building upon scheme II in [2], a more general transmission at a given time slot t writes as

$$\mathbf{s}_t = [\hat{\eta}_{t'}, 0]^T + \left[\hat{\mathbf{g}}_t^{\perp}, \hat{\mathbf{g}}_t\right] \mathbf{u}_t + \left[\hat{\mathbf{h}}_t^{\perp}, \hat{\mathbf{h}}_t\right] \mathbf{v}_t, \quad (16)$$

where $\hat{\eta}_{t'}$ can be made up of multiple overheard interferences generated at any previous slots $t'{=}\{\tau|\tau{<}t\}$. The power and rate allocated to each symbol are defined for a given quantity S as shown in Table I that represents a fraction of channel use and whose physical meaning will appear clearer in the sequel. Regarding $\mathbf{s}_t$ and the power allocated to each symbol,

Symbols	Power	Encoding Rate
$\hat{\eta}_{t'}$	$P - P^S$	$1-S$
u_1	$\frac{P^S}{2} - \frac{P^{S-\alpha_2}}{4}$	S
u_2	$\frac{P^{S-\alpha_2}}{4}$	$S-\alpha_2$
v_1	$\frac{P^S}{2} - \frac{P^{S-\alpha_1}}{4}$	S
v_2	$\frac{P^{S-\alpha_1}}{4}$	$S-\alpha_1$

TABLE I: Power and rate allocation

the received signal at each user can be written as

$$y_t = \underbrace{h_{t,1}^* \hat{\eta}_{t'}}_{P} + \underbrace{\mathbf{h}_t^H \hat{\mathbf{g}}_t^{\perp} u_{t,1}}_{P^S} + \underbrace{\mathbf{h}_t^H \hat{\mathbf{g}}_t u_{t,2}}_{P^{S-\alpha_2}} + \underbrace{\eta_{t,1}}_{P^{S-\alpha_1}} + \epsilon_{t,1}, \quad (17)$$

$$z_t = \underbrace{g_{t,1}^* \hat{\eta}_{t'}}_{P} + \underbrace{\eta_{t,2}}_{P^{S-\alpha_2}} + \underbrace{\mathbf{g}_t^H \hat{\mathbf{h}}_t^{\perp} v_{t,1}}_{P^S} + \underbrace{\mathbf{g}_t^H \hat{\mathbf{h}}_t v_{t,2}}_{P^{S-\alpha_1}} + \epsilon_{t,2}, \quad (18)$$

where $\eta_{t,1}$ and $\eta_{t,2}$ are overheard interferences received with the power $P^{S-\alpha_1}$ and $P^{S-\alpha_2}$, respectively. Both $\eta_{t,1}$ and $\eta_{t,2}$ are composed of two symbols as

$$\eta_{t,1} = \mathbf{h}_t^H \hat{\mathbf{h}}_t^{\perp} v_{t,1} + \mathbf{h}_t^H \hat{\mathbf{h}}_t v_{t,2}, \quad (19)$$

$$\eta_{t,2} = \mathbf{g}_t^H \hat{\mathbf{g}}_t^{\perp} u_{t,1} + \mathbf{g}_t^H \hat{\mathbf{g}}_t u_{t,2}. \quad (20)$$

To save the resource required by retransmission, $\eta_{t,1}$ and $\eta_{t,2}$ are quantized at the end of slot t as

$$\eta_{t,1} = \hat{\eta}_{t,1} + \tilde{\eta}_{t,1}, \quad \eta_{t,2} = \hat{\eta}_{t,2} + \tilde{\eta}_{t,2}, \quad (21)$$

where, $\hat{\eta}_{t,1}$ and $\hat{\eta}_{t,2}$ are the quantized overheard interference, $\tilde{\eta}_{t,1}$ and $\tilde{\eta}_{t,2}$ are the quantization errors. According to the Rate-distortion theory [10], we quantize $\eta_{t,1}$ and $\eta_{t,2}$ using $R_{\eta_{t,1}}$ and $R_{\eta_{t,2}}$ bits, which are equal to $(1-\alpha_1)\log P + o(\log P)$ and $(1-\alpha_2)\log P + o(\log P)$ respectively, allowing the quantization noise to have the same variances as AWGN. As a result, $\hat{\eta}_{t,1}$ and $\hat{\eta}_{t,2}$ can be employed to remove the overheard interference completely while providing an additional observation to enable the decoding of all symbols.

Moreover, $\hat{\eta}_{t'}$, decoded with rate $1-S$ by treating all the other components as noise at both receivers, can be considered as occupying $1-S$ channel use, leaving S channel use for the new symbols, $\mathbf{u}_t$ and $\mathbf{v}_t$. The number of new symbols transmitted highly depends on the value of S. If $S{>}\alpha_2$, both users will observe an overheard interference. When $\alpha_1{<}S{\leq}\alpha_2$, only $u_{t,1}$ is sent to user 1 and will be drown by the noise in z_t, thus, only one overheard interference ($\eta_{t,1}$) needs to be retransmitted. However, when $S{<}\alpha_1$, only $u_{t,1}$ and $v_{t,1}$ are transmitted and they will be drown by the noise in z_t and y_t respectively so that the transmission can finalize without the requirement of overheard interference retransmission.

Looking at the aforementioned transmission model, all the new symbols are not decodable until the transmissions of overheard interferences are completed. As a consequence, we consider all the channel uses employed to decode all the new symbols as a "virtual channel", which normally consists of

two parts: the first part is the transmission of new symbols, the second part refers to the retransmission of overheard interferences, which can boost the *DoF* from two aspects: 1) help user remove overheard interference; 2) provide an additional independent observation to enable decoding.

Next, as the limitation of the scheme in [2] lies at time slot 3, we derive the achievable scheme maintaining the transmission in the first two time slots plus the transmission of $\eta_{1,2}$ at time slot 3. Over those $3-\alpha_2$ channel uses, the *DoF* achieved by each user is $(d_1,d_2)=\left(\frac{d_{\mathbf{u}_1}+d_{u_2}}{3-\alpha_2},\frac{d_{\mathbf{v}_1}+d_{v_2}}{3-\alpha_2}\right)=\left(\frac{2+\alpha_1-\alpha_2}{3-\alpha_2},\frac{2}{3-\alpha_2}\right)$.

Moreover, as illustrated in Figure 1, the *DoF* region varies depending on the location of the intersection point. Obviously, when $2\alpha_2-\alpha_1\geq 1$, the intersection point lies on or outside the valid region formed by $d_1=1$ and $d_2=1$. The maximum sum *DoF* is obtained by the point $\left(\frac{1+\alpha_1}{2},1\right)$. When $2\alpha_2-\alpha_1<1$, the intersection point is located inside the valid region and achieves the maximum sum *DoF*. Hence, the achievable schemes are sketched in these two cases respectively.

C. Case I: $1-\Delta\leq\alpha_2$-Achieving $\left(\frac{1+\alpha_1}{2},1\right)$

Lemma 1: Assume the perfect delayed CSIT and partial current CSIT with α_1 and α_2 for each user. Under the condition $2\alpha_2-\alpha_1\geq 1$ $(1-\Delta\leq\alpha_2)$, the achievable *DoF* is $(d_1,d_2)=\left(\frac{1+\alpha_1}{2},1\right)$.

Proof: In addition to the existing two time slots of scheme II in [2] shown as (5) and (10), at time slot 3, the transmission is processed according to the scheme described in section IV-B, which is expressed in the following group of equations as

$$\mathbf{s}_3=[\hat{\eta}_{1,2},0]^T+\hat{\mathbf{g}}_3^{\perp}u_3+\left[\hat{\mathbf{h}}_3^{\perp},\hat{\mathbf{h}}_3\right]\mathbf{v}_3, \tag{22}$$

$$\mathbf{s}_4=[\hat{\eta}_{3,1},0]^T+\hat{\mathbf{g}}_4^{\perp}u_4+\left[\hat{\mathbf{h}}_4^{\perp},\hat{\mathbf{h}}_4\right]\mathbf{v}_4, \tag{23}$$

$$\mathbf{s}_5=[\hat{\eta}_{4,1},0]^T+\hat{\mathbf{g}}_5^{\perp}u_5+\left[\hat{\mathbf{h}}_5^{\perp},\hat{\mathbf{h}}_5\right]\mathbf{v}_5, \tag{24}$$

with the power and rate allocation given in Table II, where $\Delta=\alpha_2-\alpha_1$. The power of u_5 and $\mathbf{v}_5$ are not shown because

Symbols	Power	Encoding Rate
$\hat{\eta}_{1,2}$	$P-P^{\alpha_2}$	$1-\alpha_2$
u_3	$\frac{P^{\alpha_2}}{2}$	α_2
$v_{3,1}$	$\frac{P^{\alpha_2}}{2}-\frac{P^{\Delta}}{4}$	α_2
$v_{3,2}$	$\frac{P^{\Delta}}{4}$	Δ
$\hat{\eta}_{3,1}$	$P-P^{1-\Delta}$	Δ
u_4	$\frac{P^{1-\Delta}}{2}$	$1-\Delta$
$v_{4,1}$	$\frac{P^{1-\Delta}}{2}-\frac{P^{1-\Delta-\alpha_1=1-\alpha_2}}{4}$	$1-\Delta$
$v_{4,2}$	$\frac{P^{1-\alpha_2}}{4}$	$1-\alpha_2$
$\hat{\eta}_{4,1}$	$P-P^{\alpha_2}$	$1-\alpha_2$

TABLE II: Power and rate allocation for case I.

$P_{u_5}=P_{u_3}$, $P_{v_{5,1}}=P_{v_{3,1}}$ and $P_{v_{5,2}}=P_{v_{3,2}}$. As in (23) and (24), the transmission signal have the same form, the received signal at each user can be written in general as

$$y_t=\underbrace{h_{t,1}^*\hat{\eta}_{t-1,1}}_{P}+\underbrace{\mathbf{h}_t^H\hat{\mathbf{g}}_t^{\perp}u_t}_{P_{u_t}}+\underbrace{\eta_{t,1}}_{P_{\mathbf{v}_t}P^{-\alpha_1}}+\epsilon_{t,1}, \tag{25}$$

$$z_t=\underbrace{g_{t,1}^*\hat{\eta}_{t-1,1}}_{P}+\underbrace{\mathbf{g}_t^H\hat{\mathbf{h}}_t^{\perp}v_{t,1}}_{P_{v_{t,1}}}+\underbrace{\mathbf{g}_t^H\hat{\mathbf{h}}_t v_{t,2}}_{P_{v_{t,2}}}+\epsilon_{t,2}, \tag{26}$$

where $\eta_{t,1}$ is given as (19) and quantized as $\hat{\eta}_{t,1}$ via (21). Regarding the transmission flow and power allocation, two virtual channels can be established from slot 3 to 5.

1) Virtual Channel 1: This virtual channel contains the transmission of u_3, $\mathbf{v}_3$ plus $\hat{\eta}_{3,1}$. At slot 3, α_2 channel use remains after transmitting $\hat{\eta}_{1,2}$, so that one symbol, u_3, is intended to user 1 and two symbols, $v_{3,1}$ and $v_{3,2}$ to user 2. The interference overheard by user 1, $\eta_{3,1}$, has power $P_{\mathbf{v}_3}P^{-\alpha_1}=P^{\Delta}$, while user 2 overhears nothing since u_3 is drown by the noise. At the end of slot 3, $\eta_{3,1}$ is quantized as $\hat{\eta}_{3,1}$ with rate $R_{\eta_{3,1}}$ and sent using Δ channel use at slot 4.

2) Virtual Channel 2: This virtual channels consists of the transmission of u_4 and $\mathbf{v}_4$ together with $\hat{\eta}_{4,1}$. At slot 4, $1-\Delta$ channel remains for u_4 and $\mathbf{v}_4$ after transmitting $\hat{\eta}_{3,1}$. Under the condition that $1-\Delta\leq\alpha_2$, the transmitter will send only one symbol, u_4 to user 1 but two symbols, $v_{4,1}$ and $v_{4,2}$ to user 2. Consequently, $\eta_{4,1}$ is the only overheard interference at slot 4 with power $P^{1-\alpha_2}$. In each virtual channel, three new symbols and one overheard interference are transmitted. The only difference between these two virtual channels lies in the power allocation. The decodability is sketched next.

Firstly, as aforementioned, the overheard interference must be decoded first to enable the decoding procedure for the new symbols. From y_{t+1} and z_{t+1}, $\hat{\eta}_{t,1}$ is decoded by treating all the other symbols as noise. To be specific, at observation y_{t+1}, the rate of $\hat{\eta}_{t,1}$ is $I\left(\hat{\eta}_{t,1};y_{t+1}|h_{t+1,1}^*\right)=\log\frac{P}{P_{u_{t+1}}}$, while it is $I\left(\hat{\eta}_{t,1};z_{t+1}|g_{t+1,1}^*\right)=\log\frac{P}{P_{v_{t+1,1}}}$ from z_{t+1}. As shown in Table II, we let $P_{u_{t+1}}=P_{v_{t+1,1}}$, $\hat{\eta}_{t,1}$ is decoded with the same rate at both receivers. Moreover, as $\eta_{t,1}$ is seen by user 1 with power of $P_{\mathbf{v}_t}P^{-\alpha_1}$ in (25), $\hat{\eta}_{t,1}$ can completely recover $\eta_{t,1}$ provided that $\frac{P}{P_{u_{t+1}}}=P_{\mathbf{v}_t}P^{-\alpha_1}$.

Secondly, $\hat{\eta}_{t,1}$ is employed to remove the overheard interference in (25) and provide an additional independent observation for user 2. Denoting $y_t'=y_t-h_{t,1}^*\hat{\eta}_{t-1,1}$ and $z_t'=z_t-g_{t,1}^*\hat{\eta}_{t-1,1}$ as the signal after decoding and subtracting $\hat{\eta}_{t-1,1}$ from y_t and z_t respectively, we write the decoding of $\mathbf{v}_t$ and u_t as

$$y_t'-\hat{\eta}_{t,1}=\mathbf{h}_t^H\hat{\mathbf{g}}_t^{\perp}u_t+\tilde{\eta}_{t,1}+\epsilon_{t,1}, \tag{27}$$

$$\begin{bmatrix} z_t' \\ \hat{\eta}_{t,1}\end{bmatrix}=\begin{bmatrix}\mathbf{g}_t^H \\ \mathbf{h}_t^H\end{bmatrix}\left[\hat{\mathbf{h}}_t^{\perp},\hat{\mathbf{h}}_t\right]\mathbf{v}_t+\begin{bmatrix}\epsilon_{t,2} \\ -\tilde{\eta}_{t,1}\end{bmatrix}, \tag{28}$$

where $\tilde{\eta}_{t,1}$, $\epsilon_{t,1}$ and $\epsilon_{t,2}$ have unit power so that u_t is decodable with the rate of $\log P_{u_t}$ and $\mathbf{v}_t$ achieves the rate of $\log\left(P_{v_{t,1}}P_{v_{t,2}}\right)$.

Replacing the power stated in Table II, the first virtual channel lasts for $\alpha_2+\Delta$ channel uses, over which the rates achieved are $R_{u_3}=\alpha_2$ and $R_{\mathbf{v}_3}=\alpha_2+\Delta$. Similarly, they are $R_{u_4}=1-\Delta$ and $R_{\mathbf{v}_4}=2-\alpha_2-\Delta$ during the $2-\alpha_2-\Delta$ channel uses in virtual channel 2. In all, when we consider these two virtual channels which last for 2 channel uses, the *DoF* is

$$(d_1,d_2)=\left(\frac{R_{u_3}+R_{u_4}}{2},\frac{R_{\mathbf{v}_3}+R_{\mathbf{v}_4}}{2}\right)=\left(\frac{1+\alpha_1}{2},1\right). \tag{29}$$

Moreover, when the transmission continues, the amount of remaining channel uses at slot 5 is α_2, which is identical to slot 3. Repeating the same transmission results in $\eta_{5,1}$ overheard

by user 1 with the rate $R_{\eta_{5,1}}=R_{\eta_{3,1}}$, leading to $P_{u_6}=P_{u_4}$ and $P_{\mathbf{v}_6}=P_{\mathbf{v}_4}$ at slot 6. In this way, the transmission can keep cycling with the same strategy as at slot 3 and 4. Combining with the transmissions prior u_3 and $\mathbf{v}_3$ and assume the strategy is repeated for N times, the asymmetric *DoF* is given by

$$(d_1,d_2) = \lim_{N\to\infty}\left(\frac{2+\alpha_1-\alpha_2+N\times(1+\alpha_1)}{3-\alpha_2+N\times 2},\cdots \frac{2+N}{3-\alpha_2+N\times 2}\right)=\left(\frac{1+\alpha_1}{2},1\right). \quad (30)$$

□

D. Case II: $1-\Delta>\alpha_2$-Achieving $\left(\frac{2+2\alpha_1-\alpha_2}{3},\frac{2+2\alpha_2-\alpha_1}{3}\right)$

Lemma 2: Assume the transmitter has perfect delayed CSIT and partial current CSIT with α_1 and α_2 for each user. Under the condition $2\alpha_2-\alpha_1<1$ ($1-\Delta>\alpha_2$), the achievable *DoF* is $(d_1,d_2)=\left(\frac{2+2\alpha_1-\alpha_2}{3},\frac{2+2\alpha_2-\alpha_1}{3}\right)$.

Proof: To close the gap mentioned in section IV-A, we derive the achievable scheme from slot 3 (The first two slots are the same as in Case I). The transmission flow is expressed in the following group of equations as

$$\mathbf{s}_3=[\hat{\eta}_{1,2},0]^T+\hat{\mathbf{g}}_3^{\perp}u_3+\left[\hat{\mathbf{h}}_3^{\perp},\hat{\mathbf{h}}_3\right]\mathbf{v}_3, \quad (31)$$

$$\mathbf{s}_4=[\hat{\eta}_{3,1},0]^T+\left[\hat{\mathbf{g}}_4^{\perp},\hat{\mathbf{g}}_4\right]\mathbf{u}_4+\left[\hat{\mathbf{h}}_4^{\perp},\hat{\mathbf{h}}_4\right]\mathbf{v}_4, \quad (32)$$

$$\mathbf{s}_5=[\hat{\eta}_{4,1},0]^T+\hat{\mathbf{g}}_5^{\perp}u_5+\left[\hat{\mathbf{h}}_5^{\perp},\hat{\mathbf{h}}_5\right]\mathbf{v}_5, \quad (33)$$

$$\mathbf{s}_6=[\hat{\eta}_{4,2},0]^T+[\hat{\eta}_{5,1},0]^T+\hat{\mathbf{g}}_6^{\perp}u_6+\left[\hat{\mathbf{h}}_6^{\perp},\hat{\mathbf{h}}_6\right]\mathbf{v}_6, \quad (34)$$

where, $\eta_{t,1}$ and $\eta_{t,2}$, given in (19) and (20), are quantized with rate $R_{\eta_{t,1}}$ and $R_{\eta_{t,2}}$ respectively at the end of each slot via (21). Since the transmission and power allocation at slot 3 and 5 are identical to that in Table II, Table III only provides the power and the encoding rate at slot 4 and 6.

Symbols	Power	Encoding Rate
$\hat{\eta}_{3,1}$	$P-P^{1-\Delta}$	Δ
$u_{4,1}$	$\frac{P^{1-\Delta}}{2}-\frac{P^{1-\Delta-\alpha_2}}{4}$	$1-\Delta$
$u_{4,2}$	$\frac{P^{1-\Delta-\alpha_2}}{4}$	$1-\Delta-\alpha_2$
$v_{4,1}$	$\frac{P^{1-\Delta}}{2}-\frac{P^{1-\alpha_2}}{4}$	$1-\Delta$
$v_{4,2}$	$\frac{P^{1-\alpha_2}}{4}$	$1-\alpha_2$
$\hat{\eta}_{4,2}$	$P-P^{\Delta+\alpha_2}$	$1-\Delta-\alpha_2$
$\hat{\eta}_{5,1}$	$P^{\Delta+\alpha_2}-P^{\alpha_2}$	Δ
u_6	$\frac{P^{\alpha_2}}{2}$	α_2
$v_{6,1}$	$\frac{P^{\alpha_2}}{2}-\frac{P^{\Delta}}{4}$	α_2
$v_{6,2}$	$\frac{P^{\Delta}}{4}$	Δ

TABLE III: Power and rate allocation for case II (slot 4 and 6).

Regarding the transmission flow and power allocation, three virtual channels are constructed from slot 3 to 6.

1) Virtual Channel 1: This virtual channel consists of the transmission of u_3, $\mathbf{v}_3$ and $\hat{\eta}_{3,1}$. Power of u_3 and $\mathbf{v}_3$ are stated in Table II. $\mathbf{v}_3$ results in $\eta_{3,1}$, which is quantized as $\hat{\eta}_{3,1}$. The sending of $\hat{\eta}_{3,1}$ occupies Δ channel uses at slot 4. This virtual channel is identical to the first virtual channel in case I (see Section IV-C). The decodability can be derived in the same way as (25) and (26). The total amount of channel uses is $\alpha_2+\Delta$, over which the rates achieved by the symbols for each user are $R_{u_3}=\alpha_2$ and $R_{\mathbf{v}_3}=\alpha_2+\Delta$.

2) Virtual Channel 2: This virtual channel is made up of $\mathbf{u}_4$ and $\mathbf{v}_4$ and the retransmission of $\hat{\eta}_{4,1}$ and $\hat{\eta}_{4,2}$. At slot 4, the remaining amount of channel use for new symbols is $1-\Delta$, which is higher than α_2 so that the transmitter sends two symbols per user, resulting in the overheard interference $\eta_{4,1}$ and $\eta_{4,2}$ generated at user 1 and user 2 respectively. The observations at each receiver are written as

$$y_4=\underbrace{h_{4,1}^*\hat{\eta}_{3,1}}_{P}+\underbrace{\mathbf{h}_4^H\hat{\mathbf{g}}_4^{\perp}u_{4,1}}_{P_{u_{4,1}}}+\underbrace{\mathbf{h}_4^H\hat{\mathbf{g}}_4u_{4,2}}_{P_{u_{4,2}}}+\underbrace{\eta_{4,1}}_{P_{\mathbf{v}_4}P^{-\alpha_1}}+\epsilon_{4,1}, \quad (35)$$

$$z_4=\underbrace{g_{4,1}^*\hat{\eta}_{3,1}}_{P}+\underbrace{\eta_{4,2}}_{P_{\mathbf{u}_4}P^{-\alpha_2}}+\underbrace{\mathbf{g}_4^H\hat{\mathbf{h}}_4^{\perp}v_{4,1}}_{P_{v_{4,1}}}+\underbrace{\mathbf{g}_4^H\hat{\mathbf{h}}_4v_{4,2}}_{P_{v_{4,2}}}+\epsilon_{4,2}. \quad (36)$$

At the end of slot 4, $\hat{\eta}_{4,1}$ and $\hat{\eta}_{4,2}$ are obtained via quantization with rates $\log\left(P_{\mathbf{v}_4}P^{-\alpha_1}\right)$ and $\log\left(P_{\mathbf{u}_4}P^{-\alpha_2}\right)$ respectively, whose pre-log factors are $1-\alpha_2$ and $1-\Delta-\alpha_2$. The decodability of the new symbols in this virtual channel is enabled after decoding $\hat{\eta}_{4,1}$ and $\hat{\eta}_{4,2}$, which are transmitted using part of the channel at slot 4 and 5 respectively. The received signals of user 1 at slot 5 and 6 are expressed as

$$y_5=\underbrace{h_{5,1}^*\hat{\eta}_{4,1}}_{P}+\underbrace{\mathbf{h}_5^H\hat{\mathbf{g}}_5^{\perp}u_5}_{P_{u_5}}+\underbrace{\eta_{5,1}}_{P_{\mathbf{v}_5}P^{-\alpha_1}}+\epsilon_{5,1}, \quad (37)$$

$$y_6=\underbrace{h_{6,1}^*\hat{\eta}_{4,2}}_{P}+\underbrace{h_{6,1}^*\hat{\eta}_{5,1}}_{P^{\Delta+\alpha_2}}+\underbrace{\mathbf{h}_6^H\hat{\mathbf{g}}_6^{\perp}u_6}_{P_{u_6}}+\underbrace{\eta_{6,1}}_{P_{\mathbf{v}_6}P^{-\alpha_1}}+\epsilon_{6,1}. \quad (38)$$

By treating all the other symbols as noise, $\hat{\eta}_{4,1}$ is obtained with the rate of $I\left(\hat{\eta}_{4,1};y_5|h_{5,1}^*\right)=\log\frac{P}{P_{u_5}}$. Revisiting Table II, $P_{u_5}=P_{u_3}=P^{\alpha_2}$ so that $\hat{\eta}_{4,1}$ is decodable with rate $1-\alpha_2$ and $\eta_{4,1}$ can be successfully recovered. Similarly, $\hat{\eta}_{4,2}$ is decoded from y_6 by treating all the other symbols as noise, among which, $\hat{\eta}_{5,1}$ is the dominant component. Consequently, $\hat{\eta}_{4,2}$ is decoded with the rate of $I\left(\hat{\eta}_{4,2};y_6|h_{6,1}^*\right)=\log\frac{P}{P_{\hat{\eta}_{5,1}}}$, which meets its distortion rate $1-\Delta-\alpha_2$. Similarly, $\hat{\eta}_{4,1}$ and $\hat{\eta}_{4,2}$ are decoded from z_5 and z_6 respectively. Denoting $y_4'=y_4-h_{4,1}^*\hat{\eta}_{3,1}$ and $z_4'=z_4-g_{4,1}^*\hat{\eta}_{3,1}$, the decoding formulas for $\mathbf{u}_4$ and $\mathbf{v}_4$ are

$$\begin{bmatrix} y_4'-\hat{\eta}_{4,1}\\ \hat{\eta}_{4,2}\end{bmatrix}=\begin{bmatrix}\mathbf{h}_4^H\\ \mathbf{g}_4^H\end{bmatrix}\left[\hat{\mathbf{g}}_4^{\perp},\hat{\mathbf{g}}_4\right]\mathbf{u}_4+\begin{bmatrix}\tilde{\eta}_{4,1}+\epsilon_{4,1}\\ -\tilde{\eta}_{4,2}\end{bmatrix}, \quad (39)$$

$$\begin{bmatrix} z_4'-\hat{\eta}_{4,2}\\ \hat{\eta}_{4,1}\end{bmatrix}=\begin{bmatrix}\mathbf{g}_4^H\\ \mathbf{h}_4^H\end{bmatrix}\left[\hat{\mathbf{h}}_4^{\perp},\hat{\mathbf{h}}_4\right]\mathbf{v}_4+\begin{bmatrix}\tilde{\eta}_{4,2}+\epsilon_{4,2}\\ -\tilde{\eta}_{4,1}\end{bmatrix}, \quad (40)$$

where $\tilde{\eta}_{4,1}$, $\tilde{\eta}_{4,2}$, $\epsilon_{4,1}$ and $\epsilon_{4,2}$ have unit power, $\mathbf{u}_4$ and $\mathbf{v}_4$ can be decoded with the rate of $\log P_{\mathbf{u}_4}$ and $\log P_{\mathbf{v}_4}$, respectively, which equal their encoding rate. As a result, virtual channel 2 lasts for $3-2\alpha_2-2\Delta$ channel uses while the rate achieved are $R_{\mathbf{u}_4}=2-2\Delta-\alpha_2$ and $R_{\mathbf{v}_4}=2-\Delta-\alpha_2$.

3) Virtual Channel 3: This virtual channel contains the transmissions of u_5, $\mathbf{v}_5$ and $\hat{\eta}_{5,1}$. As the transmission and power allocation of u_5 and $\mathbf{v}_5$ are identical to that at slot 3, $\eta_{5,1}$ is quantized with the rate Δ. After subtracting $\hat{\eta}_{4,2}$ from (38), $\hat{\eta}_{5,1}$ is decoded by treating the rest as noise, among which, u_6 is the dominant. The decoding rate of $\hat{\eta}_{5,1}$

is $I\left(\hat{\eta}_{5,1}; y_6 | h^*_{6,1}, \hat{\eta}_{4,2}\right) = \log \frac{P_{\hat{\eta}_{5,1}}}{P_{u_6}}$, whose pre-log factor is Δ. Consequently, $\hat{\eta}_{5,1}$ can be employed to remove the interference in y_5 and provide an additional observation to z_5. In this way, u_5 and $\mathbf{v}_5$ can be decoded using (25) and (26). The rates achieved are $R_{u_5}=\alpha_2$ and $R_{\mathbf{v}_5}=\alpha_2+\Delta$ over the $\alpha_2+\Delta$ channel use.

In all, looking at those three virtual channels which last for 3 channel uses in total, the *DoF* achieved are expressed as

$$\begin{aligned}(d_1, d_2) &= \frac{\left(R_{u_3} + R_{\mathbf{u}_4} + R_{u_5}, R_{\mathbf{v}_3} + R_{\mathbf{v}_4} + R_{\mathbf{v}_5}\right)}{2\left(\alpha_2 + \Delta\right) + 3 - 2\alpha_2 - 2\Delta} \\ &= \left(\frac{2 + 2\alpha_1 - \alpha_2}{3}, \frac{2 + 2\alpha_2 - \alpha_1}{3}\right). \end{aligned} \tag{41}$$

Combining with the *DoF* prior to u_3 and $\mathbf{v}_3$ and cycling those three virtual channels for N times, the achievable *DoF* is

$$\begin{aligned}(d_1, d_2) = \lim_{N\to\infty} \Bigg(&\frac{2 + \alpha_1 - \alpha_2 + N \times 3 d_1}{3 - \alpha_2 + N \times 3}, \cdots \\ &\frac{2 + N \times 3 d_2}{3 - \alpha_2 + N \times 3}\Bigg) = \left(\frac{2 + 2\alpha_1 - \alpha_2}{3}, \frac{2 + 2\alpha_2 - \alpha_1}{3}\right).\end{aligned}$$

□

E. Case II: $1-\Delta>\alpha_2$-Achieving $(\alpha_2, 1)$

Point $(\alpha_2, 1)$ is achieved under the condition that $1-\Delta>\alpha_2$ as in case I but by reusing the flow described in Section IV-C. The first virtual channel is maintained, where u_3 and $\mathbf{v}_3$ achieve the rate of α_2 and $\alpha_2+\Delta$ respectively and consume $\alpha_2+\Delta$ channel uses. However, the second virtual channel is changed by reallocating the power of u_4 from $P^{1-\Delta}$ to P^{α_2}. In this way, the amount of channel uses in this virtual channel is kept to $2-\Delta-\alpha_2$, while the rates achieved become $R_{u_4}=\alpha_2$ and $R_{\mathbf{v}_4}=2-\Delta-\alpha_2$. As a result, the *DoF* achieved using this 2 channel uses are $(d_1,d_2)=(\alpha_2,1)$.

F. Achieving $(1, \alpha_1)$

Point $(1, \alpha_1)$ is achieved in a "SC+ZF" manner which has been mentioned in [2]. The transmission scheme is finished in one slot and is expressed as

$$\mathbf{s}_t = [x_{c,t}, 0]^T + \hat{\mathbf{g}}_t^{\perp} u_t + \hat{\mathbf{h}}_t^{\perp} v_t, \tag{42}$$

where $x_{c,t}$ is intended to user 1 and transmitted with power P superposed to u_t and v_t, which are transmitted with power P^{α_1}. u_t and v_t are precoded to the orthogonal space of the channel of their unintended user. At each receiver, $x_{c,t}$ is decoded with the rate of $1-\alpha_1$ using SIC. After subtracting $x_{c,t}$, user 1 decodes u_t with the rate of α_1 without any interference. Similarly, user 2 obtains v_t with *DoF* of α_1. Resultantly, point $(1, \alpha_1)$ is achieved.

As a last remark, we note the similarity of this work with [9], where the same *DoF* region is derived under the same system settings. Their achievable scheme in terminated in three phases. The overheard interferences generated in current phase are accumulated and then split evenly across the transmission in the next phase. The optimal bound is achieved by choosing phase durations which optimally combine the transmission of overheard interference and new symbols. However, in this contribution, we achieved the optimal bound by keeping retransmitting overheard interference to boost up the *DoF* and making every channel use employed efficiently.

V. Conclusion

The optimal *DoF* region is derived for a two-user MISO broadcast channel when the transmitter has perfect delayed CSI and asymmetric partial current CSI. A novel transmission scheme is motivated and shown to achieve that *DoF* region. The results boil down to [1], [2], [3] in the symmetric scenario.

Appendix-Brief Proof of Outer-Bound

The converse proposed in [2] can be reused to prove the optimal region given in Theorem 1. In that work, genie-aided model is employed to construct a physically-degraded channel. Skipping the same fundamental steps, the only difference lies in deriving the following lower bound

$$\begin{aligned}&\mathcal{E}_{\tilde{\phi}}\left(\log\left(1 + \sum_{i=1}^{m} \lambda_i |\hat{\phi}_i + \tilde{\phi}_i|^2\right)\right) \\ \geq &\mathcal{E}_{\tilde{\phi}_1}\left(\log\left(\lambda_1 |\tilde{\phi}_1|^2\right)\right) \\ \approx &\log \lambda_1 \sigma_2^2 = (1 - \alpha_2)\log P. \end{aligned} \tag{43}$$

$\lambda_1>\lambda_2>\cdots>\lambda_m$ are eigenvalues of $\hat{\mathbf{g}}$. $\hat{\phi}_i+\tilde{\phi}_i$ are eigenvalues of $\mathbf{g}$, $\tilde{\phi}$ is Gaussian distributed as $\mathcal{N}\left(0,\sigma_2^2\right)$. Replacing (43) into its corresponding equations in [2], we have (44). When switching the role of the two users, (45) is obtained.

$$R_1 + 2R_2 \leq (2 + \alpha_2)\log P, \tag{44}$$

$$2R_1 + R_2 \leq (2 + \alpha_1)\log P. \tag{45}$$

References

[1] M. Maddah-Ali and D. Tse, "Completely stale transmitter channel state information is still very useful," *IEEE Trans. Inf. Theory*, vol. 58, no. 7, pp. 4418–4431, 2012.

[2] S. Yang, M. Kobayashi, D. Gesbert, and X. Yi, "Degrees of freedom of time correlated miso broadcast channel with delayed csit," *IEEE Trans. Inf. Theory*, no. 99, p. 14, 2012.

[3] T. Gou and S. Jafar, "Optimal use of current and outdated channel state information: Degrees of freedom of the miso bc with mixed csit," *Comms Letters, IEEE*, vol. 16, no. 7, pp. 1084 –1087, july 2012.

[4] C. Vaze and M. Varanasi, "The degrees of freedom region of the two-user mimo broadcast channel with delayed csit," in *Proc. IEEE Int. Symp. Inf. Theory (ISIT)*, 31 2011-aug. 5 2011, pp. 199 –203.

[5] ——, "The degree-of-freedom regions of mimo broadcast, interference, and cognitive radio channels with no csit," *IEEE Trans. Inf. Theory,*, vol. 58, no. 8, pp. 5354 –5374, aug. 2012.

[6] C. Huang, S. Jafar, S. Shamai, and S. Vishwanath, "On degrees of freedom region of mimo networks without channel state information at transmitters," *IEEE Trans. Inf. Theory*, vol. 58, no. 2, pp. 849 –857, feb. 2012.

[7] H. Maleki, S. Jafar, and S. Shamai, "Retrospective interference alignment over interference networks," *IEEE Journal of Selected Topics in Signal Processing*, vol. 6, no. 3, pp. 228 –240, june 2012.

[8] R. Tandon, M. Maddah-Ali, A. Tulino, H. Poor, and S. Shamai, "On fading broadcast channels with partial channel state information at the transmitter," in *9th Int. Symp. on Wireless Communication Systems*, Paris, France, Aug. 2012.

[9] J. Chen and P. Elia, "Degrees-of-freedom region of the miso broadcast channel with general mixed-csit," vol. arxiv/1205.3474, May, 2012.

[10] T. M. Cover and J. A. Thomas, *"Elements of Information Theory, second edition*. New York: Wiley-Intersicence, 2006.